HHS Public Access

Author manuscript

Macromol Mater Eng. Author manuscript; available in PMC 2017 October 20.

Published in final edited form as:

Macromol Mater Eng. 2017 May ; 302(5): . doi:10.1002/mame.201600487.

Engineered Peptide Repairs Defective Adhesive–Dentin Interface

Dr. Qiang Ye,
Bioengineering Research Center (BERC), University of Kansas (KU), 1530 W. 15th St, Lawrence, KS 66045, USA

Prof. Paulette Spencer,
Bioengineering Research Center (BERC), University of Kansas (KU), 1530 W. 15th St, Lawrence, KS 66045, USA. Department of Mechanical Engineering, University of Kansas (KU), 1530 W. 15th St, Lawrence, KS 66045, USA

Dr. Esra Yuca, and
Bioengineering Research Center (BERC), University of Kansas (KU), 1530 W. 15th St, Lawrence, KS 66045, USA

Prof. Candan Tamerler
Bioengineering Research Center (BERC), University of Kansas (KU), 1530 W. 15th St, Lawrence, KS 66045, USA. Department of Mechanical Engineering, University of Kansas (KU), 1530 W. 15th St, Lawrence, KS 66045, USA

Abstract

Failure of dental composite restorations is primarily due to recurrent decay at the tooth–composite interface. At this interface, the adhesive and its bond with dentin is the barrier between the restored tooth and the oral environment. In vivo degradation of the bond formed at the adhesive/dentin (a/d) interface follows a cascade of events leading to weakening of the composite restoration. Here, a peptide-based approach is developed to mineralize deficient dentin matrices at the a/d interface. Peptides that have an inherent capacity to self-assemble on dentin and to induce calcium–phosphate remineralization are anchored at the interface. Distribution of adhesive, collagen, and mineral is analyzed using micro-Raman spectroscopy and fluorescence microscopy. The analysis demonstrates remineralization of the deficient dentin matrices achieved throughout the interface with homogeneous distribution of mineral. The peptide-based remineralization demonstrated here can be an enabling technology to design integrated biomaterial–tissue interfaces.

Graphical abstract

Correspondence to: Candan Tamerler.

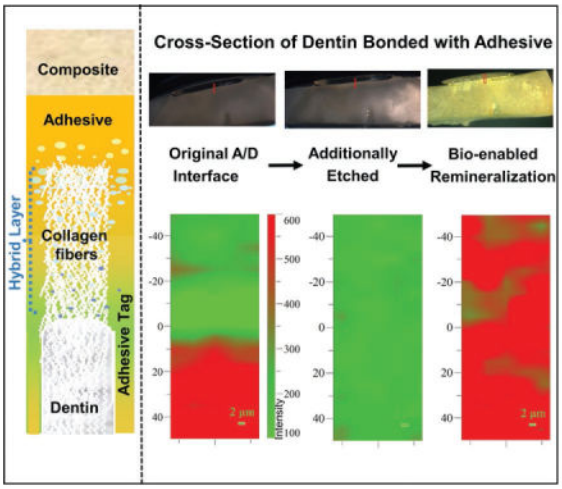

Keywords

adhesive/dentin interface; composite restorative materials; material–tissue interface; mineralization; peptides

1. Introduction

Resin-based composite is the most popular material for direct restorative dentistry, but the clinical lifetime of composite restorations may be limited to 5.7 years[1–3] and patients at highest risk for decay are particularly vulnerable to early failure.[1,4] The primary reason composite restorations fail is recurrent caries, i.e., carious lesions on the margins of existing restorations.[5] The margins between the composite material and tooth structure are marked by deficiencies and discrepancies. These marginal defects are clear evidence that there is not an effective seal at the composite/tooth interface.

The viscous composite material is not bonded directly to the tooth—a low-viscosity adhesive is used to connect the composite to the tooth (enamel and dentin). Adhesive bonding to enamel has been successful, but a variety of factors lead to failure of the bond between adhesive and dentin. These factors include endogenous enzymes, e.g., matrix metalloproteinases that degrade exposed demineralized dentin; bacterial and salivary enzymes degrade the adhesive; chemical as well as enzymatic hydrolysis degrades the adhesive/dentin (a/d) bond.[6] Bacteria penetrate the degraded interface, cariogenic plaque accumulates within the exposed, demineralized dentin, and decay is unavoidable, as demonstrated by clinical studies.[7–10]

The fundamental processes involved in bonding an adhesive to dentin are removal of the mineral phase without altering the collagen and filling the voids left by the mineral with adhesive that undergoes complete in situ polymerization. The demineralized dentin collagen that is infiltrated and reinforced by adhesive is known as the hybrid layer. The hybrid layer has been called the weakest link in the adhesive–dentin bond.[7] Indeed, failure of the a/d bond occurs via fracture through the resin tags as well as through the hybrid layer.[11,12] The

relationship of the a/d bond to the hybrid layer is shown in Scheme 1. As noted in this figure, adhesive infiltration decreases toward the dentin matrix portion of the hybrid layer.

Establishing and maintaining the integrity of the a/d bond has been a formidable challenge. Failure of this bond has been a major contributor to the limited clinical lifetime of composite restorations. Peptide-mediated remineralization of deficient dentin matrices within the a/d interface offers promise as a viable solution to this problem. The remineralized matrices could provide critical integrity to the a/d interface; they could offer interfacial integration. The remineralized matrices could reinforce the a/d interfacial bond and the ability of this bond to act as a barrier between the repaired tooth and the oral environment.

Proteins that mediate biomineralization events offer a guide for understanding how to manipulate the deposition of calcium phosphate compounds to treat mineralized tissues. They contribute to regulation of the balance between ionic saturation and mineral precipitation by providing spatial and temporal control of ion transport to the mineralization front.[13–16] They can also template the nucleation and growth processes by acting as heterogeneous nucleation sites or by specific interactions with the crystal surface. For example, dentin matrix protein (DMP) 1 plays an important role in mineralized tissue formation by initiation of nucleation through stabilization of calcium and phosphate ions in solution.[17] These prenucleation clusters may result in formation of amorphous calcium phosphate following crystal growth in the intrafibrillar gap zones of collagen molecules.[18–20] Similarly, amelogenin, a protein found in developing tooth enamel, regulates initiation and growth of hydroxyapatite crystals during mineralization of enamel.[21–23]

Although several proteins are related to biomineralization, utilization of these proteins in tissue repair can be daunting due to the complexity of events and the number of proteins that are involved in the process.[24,25] The relatively shorter peptide sequences that mimic the role of natural proteins may allow for better control. Our group has been investigating biocombinatorially selected peptides that have specific affinities to minerals.[16,26,27] We have identified peptides that are specific to hydroxyapatite mineral and demonstrated that these peptides mediate amorphous calcium phosphate mineralization.[16] We also demonstrated that hydroxyapatite specific peptides when coupled with another peptide having gel forming property result in biological-like apatite formation in the peptide-hydrogel matrix.[16,28] Using hydroxyapatite specific peptides, we next designed amelogenin protein-derived peptides that promote rapid nucleation of calcium/phosphate to remineralize artificial root caries in vitro.[15] Recently, DMP-derived peptides that bind to collagen were demonstrated to promote remineralization of human dentin.[29] A collagen/calcium dual-affinitive peptide having a high affinity for dentin collagen matrix was shown to seal dentin tubules.[30]

We have fused hydroxyapatite binding peptide (HABP) to N-terminus of a green fluorescence protein variant (GFPuv) to produce GFPuv–HABP chimeric protein. GFPuv–HABP has been characterized and demonstrated as a fluorescence probe to mark biomineralized materials and tissues.[31] GFPuv–HABP has also been incorporated into binary blend fibers to obtain bioactive shape memory fibers.[32]

Given that these peptides, which are biocombinatorially selected or computationally derived from natural proteins, recognize and bind to different biominerals, in this work we explored the inherent capability of a peptide-based approach to design an integrated material–tissue interface. An engineered hydroxyapatite specific peptide was utilized to remineralize deficient dentin matrices by self-anchoring the peptide to the a/d interface (Scheme 1). Our results demonstrate, for the first time, that a peptide-mediated approach resulted in extensive remineralization throughout the a/d interface, a major step toward preventing recurrent decay at the margins of composite restorations.

2. Experimental Section

2.1. Materials

2,2-Bis[4-(2-hydroxy-3-methacryloxypropoxy)phenyl]propane (BisGMA) and 2-hydroxyethyl methacrylate (HEMA) were obtained from Sigma-Aldrich (St. Louis, MO, USA) and used without further purification as comonomers. Camphorquinone (CQ), ethyl-4-(dimethylamino)benzoate (EDMAB), and diphenyliodonium hexafluorophosphate (DPIHP) were obtained from Sigma-Aldrich (St. Louis, MO). All other chemicals were reagent grade and used without further purification.

2.2. Preparation of Adhesive/Dentin Specimens

The a/d interface specimens were prepared using published protocols.[7,33] Three extracted unerupted human third molars, stored at 4 °C in 0.9% w/v NaCl containing 0.002% sodium azide, were used. The occlusal 1/3 of the crown was sectioned perpendicular to the long axis of a molar. The exposed dentin surface was etched for 60 s with 35% phosphoric acid, rinsed with water and excess superficial water was removed. The protocol was not identical to clinical treatment. Particularly, challenging experimental conditions were chosen for this model system as the shorter etching time would likely lead to modest demineralization. With the longer etching time, extensive demineralization of the dentin was achieved. The adhesive formulation, which is a mimic of commercial dentin adhesives, consisted of HEMA and BisGMA 45/55 wt% and three-component photoinitiator system, i.e., CQ (0.5 mol%), EDMAB (0.5 mol%), and DPIHP (1.0 mass%). Additionally, adhesive composition contained 20 mass% ethanol.[34–36] Consecutive coats of adhesive were applied, polymerized by visible light and the specimens were dark-cured for 48 h. The treated dentin surfaces were sectioned perpendicular and parallel to the bonded surface. The resultant a/d interface specimens were characterized using micro-Raman spectroscopy (μRS). The specimens were remineralized using the protocol described in Section 2.3.

2.3. Remineralization Studies

HABP coupled to GFP was absorbed on the a/d interface. The HABP with a sequence of CMLPHHGAC was previously selected using phage display protocols. By using a GFP derivative (GFPuv) as a tag, HABP was engineered as a bifunctional fluorescent probe. The remineralization reaction was initiated by an alkaline phosphatase (AP, Thermo Scientific) at a final concentration of 1.4×10^{-6} g mL^{-1}. In this reaction, AP hydrolyzes the organic phosphate compound to PO_4^{-3}. The mineralization solution (2×) was prepared using 48×10^{-3} M $CaCl_2$ and 28.8×10^{-3} M β-glycerophosphate in 50×10^{-3} M Tris-HCl buffer. The

tooth sample was incubated with 400 × 10^{-6} M GFP–HABP protein, mineralization solution and AP for 24 h at 37 °C with continuous shaking at 100 rpm. Following the completion of the reaction, the samples were washed with sterile water for 1 h, dried, and examined using fluorescent microscopy and μRS.

2.4. Characterization of Specimen

The a/d interface specimens were imaged using μRS to determine the distribution of adhesive, collagen, and mineral based on the representative molecular groups. A LabRAM ARAMIS Raman spectrometer (LabRAM HORIBA Jobin Yvon, Edison, NY) was used with an HeNe laser (λ = 633 nm, a laser power of 17 mW) as an excitation source. The instrument parameters were: 200 μm confocal hole, 150 μm wide entrance slit, 600 g mm^{-1} grating, and 100× objective Olympus lens. The samples were mounted on a computer-controlled, high-precision *x*–*y* stage, and Raman spectra were acquired over a range of 700–1800 cm^{-1}. Processing of the Raman spectral data was performed using LabSPEC 5 software (HORIBA Jobin Yvon, Edison, NJ).

Following initial μRS analysis, the exposed a/d interface was treated for 20 s with 5% NaOCl followed by 5 N HCl for 30 min. After this treatment, the a/d specimens were functionalized by GFP–HABP by simply dipping into protein suspension allowing HABP to self-anchor. The excess protein was removed by washing. Remineralized samples were monitored using a fluorescence microscope equipped with a 4× objective on a plate reader (Cytation3, BioTek, Winooski, VT, USA). The remineralized samples were also analyzed using μRS.

3. Results and Discussion

The prepared specimens were composed of dentin bonded with adhesive. These specimens were cut, as described above, to provide a/d interface samples that were treated with HABP. The peptide was coupled with a GFP–HABP to facilitate our ability to monitor the peptide during fluorescent microscopic imaging of the samples. The peptide has an inherent capacity to self-assemble on dentin and to induce remineralization of defective dentin matrices at the a/d interface. Micro-Raman spectroscopic imaging was used to analyze the molecular structure and to determine the distribution of adhesive, collagen and mineral across the a/d interface before and after remineralization.

The HABP peptide was selected biocombinatorially using a phage display library and the peptide demonstrated distinctive ability to induce mineralization with morphological control.[16] In previous studies, we demonstrated that the HABP peptides genetically engineered to couple with GFPuv eased the monitoring of the selective binding abilities of peptide on different biomineral and calcium phosphate coated implant materials.[31,37] Here the peptides coupled with GFP were anchored at the a/d interface by simply dipping the prepared specimens into the protein solution. Samples were washed extensively to remove excessive protein on the specimens. Remineralization is initiated using enzyme-based assay mimicking biological systems by incorporating alkaline phosphatase enzyme. Here enzyme-based mineralization offers control of the kinetics by controlling the phosphate ion release from the organic phosphate source cleaved by alkaline phosphatase.[18] Figure 1 shows the

prepared a/d specimens prior to and after etching (Figure 1a–c). The fluorescence protein assembly on the samples (Figure 1d) provided to monitor the homogeneous protein coverage and remineralization of the samples (Figure 1e–h).

The molecular structure of the a/d interface specimens was determined using confocal micro-Raman microspectroscopy. The Raman spectrum provides a “fingerprint” of the molecules present within the a/d interface. The technique can be used for both qualitative and quantitative determination. For example, the representative Raman spectrum of dentin (Scheme 1) reveals features associated with the mineral and collagen matrix. The Raman spectral features at 962 and 1070 cm^{-1} are associated with dentin mineral phosphate (PO_4^{-3}) and carbonate (CO_3^{-2}), respectively. Spectral features associated with dentin collagen matrix are 1671 cm^{-1} (amide I) and 1464 cm^{-1} (CH_2).

The 2D Raman *XY* imaging provided a distinctive representation of the distribution of adhesive (colored as green) and mineral (colored as red) across the a/d interface (Figure 2a). The spectra in the 2D Raman *XY* image were collected from points on the specimen, which are separated by 1 μm. The series of line mapping spectra (Figure 2b) were acquired at 1 μm intervals across the original a/d interface. Based on both visual and spectroscopic examination, the spectra from position −5 to 5 μm were acquired from pure adhesive. Vibrational bands associated with the adhesive and collagen components of dentin are noted in the spectra at position 5–15 μm. The relative increase in the intensity of the 962 cm^{-1} band (P–O symmetric stretch) at ≈15 μm suggests that this spectrum represents the bottom of the demineralized dentin; this conclusion is supported by our previous publications.[38,39] Following the initial μRS analysis, the exposed a/d interface was treated with NaOCl followed by HCl demineralization. The extent of dentin demineralization was determined by analyzing the relative intensities of the spectral features associated with mineral and collagen (Figure 3a,b). Following treatment of the specimens with HCl, spectral features associated with the mineral (e.g., PO_4^{-2} at 962 cm^{-1}) were absent while the spectral features associated with collagen 1671 cm^{-1} (amide I) and 1464 cm^{-1} (CH_2) were detectable. Raman *XY* imaging confirmed the presence of adhesive (Figure 3a).

Spectral analysis of the specimen following peptide-mediated remineralization demonstrated a major increase in the intensity of the peak at 962 cm^{-1}. This increase confirms the presence of the P–O group at the a/d interface (Figure 3c,d). Raman *XY* imaging confirms the distribution of mineral achieved throughout the a/d interface. Since μRS is nondestructive, the specimens were also imaged using fluorescent microscopy. Both adhesive and dentin have the fluorescent property following the remineralization reaction (Figure 2e,f), confirming GFP–HABP as integral components of the integrated adhesive/dentin interface. These complementary analyses provide clear evidence of peptide-mediated remineralization of deficient dentin matrices at the a/d interface.

4. Conclusions

Recurrent decay at the composite/tooth margin is the primary reason for failure of composite restorations. At these vulnerable margins, the adhesive and its bond to dentin can be the barrier between the repaired tooth and the surrounding oral environment. A failed adhesive/

dentin bond means that there are crevices at the composite/tooth margin, pathogens can infiltrate these crevices and undermine the composite restoration. The lack of a durable adhesive/dentin bond is considered one of the major problems with the use of composites in direct restorative dentistry. We addressed this problem using an engineered hydroxyapatite specific peptide to remineralize deficient dentin matrices. The peptide, anchored at the interface, induced remineralization to provide an integrated adhesive/dentin interfacial bond. Our results show, for the first time, a peptide-mediated approach to improve deficiencies at the adhesive/dentin interface. This enabling technology could be applicable to a wide range of interfacial structures, e.g., biomaterial–tissue interfaces, where integration of dissimilar materials is required to restore form and function to tissues damaged by disease, age, or trauma.

Acknowledgments

This investigation was supported by Research Grants R01 DE022054 and R01 DE025476 from the National Institute of Dental and Craniofacial Research, National Institutes of Health, Bethesda, MD 20892, USA.

References

1. DeRouen TA, Martin MD, Leroux BG, Townes BD, Woods JS, Leitao J, Castro-Caldas A, Luis H, Bernardo M, Rosenbaum G, Martins IP. JAMA, J Am Med Assoc. 2006; 295:1784.
2. Ferracane JL. Dent Mater. 2013; 29:51. [PubMed: 22809582]
3. Simecek JW, Diefenderfer KE, Cohen ME. J Am Dent Assoc. 2009; 140:200. [PubMed: 19188417]
4. van de Sande FH, Opdam NJ, Rodolpho PAD, Correa MB, Demarco FF, Cenci MS. J Dent Res. 2013; 92:S78.
5. Bernardo M, Luis H, Martin MD, Leroux BG, Rue T, Leitao J, DeRouen TA. J Am Dent Assoc. 2007; 138:775. [PubMed: 17545266]
6. Ferracane JL, Hilton TJ. Dent Mater. 2016; 32:1. [PubMed: 26220776]
7. Spencer P, Ye Q, Park J, Topp EM, Misra A, Marangos O, Wang Y, Bohaty BS, Singh V, Sene F, Eslick J, Camarda K, Katz JL. Ann Biomed Eng. 2010; 38:1989. [PubMed: 20195761]
8. Svanberg M, Mjor IA, Orstavik D. J Dent Res. 1990; 69:861. [PubMed: 2109000]
9. Opdam NJM, Bronkhorst EM, Loomans BAC, Huysmans M. J Dent Res. 2010; 89:1063. [PubMed: 20660797]
10. Leinfelder KF. J Am Dent Assoc. 2000; 131:1186. [PubMed: 10953536]
11. Sano H, Yoshikawa T, Pereira PNR, Kanemura N, Morigami M, Tagami J, Pashley DH. J Dent Res. 1999; 78:906. [PubMed: 10326735]
12. Soappman MJ, Nazari A, Porter JA, Arola D. Dent Mater. 2007; 23:608. [PubMed: 16806452]
13. Simmer JP, Fincham AG. Crit Rev Oral Biol Med. 1995; 6:84. [PubMed: 7548623]
14. Hunter GK, Goldberg HA. Proc Natl Acad Sci USA. 1993; 90:8562. [PubMed: 8397409]
15. Gungormus M, Oren EE, Horst JA, Fong H, Hnilova M, Somerman MJ, Snead ML, Samudrala R, Tamerler C, Sarikaya M. Int J Oral Sci. 2012; 4:69. [PubMed: 22743342]
16. Gungormus M, Fong H, Kim IW, Evans JS, Tamerler C, Sarikaya M. Biomacromolecules. 2008; 9:966. [PubMed: 18271563]
17. Dey A, Bomans PHH, Muller FA, Will J, Frederik PM, de With G, Sommerdijk N. Nat Mater. 2010; 9:1010. [PubMed: 21076415]
18. Kim J, Arola DD, Gu LS, Kim YK, Mai S, Liu Y, Pashley DH, Tay FR. Acta Biomater. 2010; 6:2740. [PubMed: 20045745]
19. Niu LN, Jiao K, Ryou H, Diogenes A, Yiu CKY, Mazzoni A, Chen JH, Arola DD, Hargreaves KM, Pashley DH, Tay FR. Biomacromolecules. 2013; 14:1661. [PubMed: 23586938]
20. Tay FR, Pashley DH. Biomaterials. 2008; 29:1127. [PubMed: 18022228]

21. Snead ML, Zhu D, Lei Y, White SN, Snead CM, Luo W, Paine ML. Mater Sci Eng, C-Bio S. 2006; 26:1296.
22. Du C, Falini G, Fermani S, Abbott C, Moradian-Oldak J. Science. 2005; 307:1450. [PubMed: 15746422]
23. Bartlett JD, Ganss B, Goldberg M, Moradian-Oldak J, Paine ML, Snead ML, Wen X, White SN, Zhou YL. Curr Top Dev Biol. 2006; 74:57. [PubMed: 16860665]
24. Lowenstam HA. Science. 1981; 211:1126. [PubMed: 7008198]
25. Addadi L, Weiner S. Proc Natl Acad Sci USA. 1985; 82:4110. [PubMed: 3858868]
26. Tamerler C, Sarikaya M. ACS Nano. 2009; 3:1606. [PubMed: 21452861]
27. Tamerler C, Khatayevich D, Gungormus M, Kacar T, Oren EE, Hnilova M, Sarikaya M. Biopolymers. 2010; 94:78. [PubMed: 20091881]
28. Gungormus M, Branco M, Fong H, Schneider JP, Tamerler C, Sarikaya M. Biomaterials. 2010; 31:7266. [PubMed: 20591477]
29. Padovano JD, Ravindran S, Snee PT, Ramachandran A, Bedran-Russo AK, George A. J Dent Res. 2015; 94:608. [PubMed: 25694469]
30. Wang RH, Wang Q, Wang XM, Tian LL, Liu HY, Zhao MM, Peng C, Cai Q, Shi YM. J Biomater Appl. 2014; 29:268. [PubMed: 24505078]
31. Yuca E, Karatas AY, Seker UOS, Gungormus M, Dinler-Doganay G, Sarikaya M, Tamerler C. Biotechnol Bioeng. 2011; 108:1021. [PubMed: 21190171]
32. Wu X, Mahalingam S, VanOosten SK, Wisdom C, Tamerler C, Edirisinghe M. Macromol Biosci. 2016; 17:1600270.
33. Spencer P, Wang Y. J Biomed Mater Res. 2002; 62:447. [PubMed: 12209931]
34. Ye Q, Park JG, Topp E, Wang Y, Misra A, Spencer P. J Dent Res. 2008; 87:829. [PubMed: 18719208]
35. Ye Q, Park J, Topp E, Spencer P. Dent Mater. 2009; 25:452. [PubMed: 19027937]
36. Ye Q, Park J, Laurence JS, Parthasarathy R, Misra A, Spencer P. J Dent Res. 2011; 90:1434. [PubMed: 21960682]
37. Utku FS, Yuca E, Seckin E, Goller G, Karatas AY, Urgen M, Tamerler C. Bioinspired, Biomimetic Nanobiomater. 2015; 4:155.
38. Wang Y, Spencer P. J Biomed Mater Res. 2002; 60:300. [PubMed: 11857437]
39. Wang Y, Spencer P. J Biomed Mater Res, Part A. 2005; 75A:580.
40. Misra A, Spencer P, Marangos O, Wang Y, Katz JL. J Biomed Mater Res, Part B Appl Biomater. 2004; 70:56. [PubMed: 15199584]

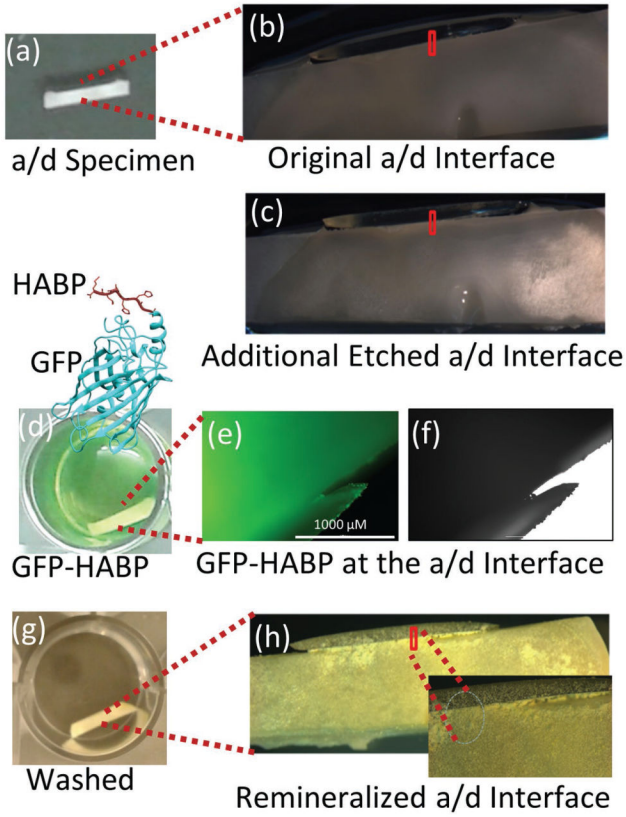

Figure 1.

Representative visible images to show the enlarged region from the adhesive/dentine interface. a,b) Original a/d interface. c) Additional etched a/d interface. d) Remineralization of the specimen by GFP-HABP. e,f) GFP-HABPs surface coverage by FM analysis. g) Extensively washed adhesive/dentin-specimen to remove excessive unbound protein. h) Mineralization a/d interface after remineralization.

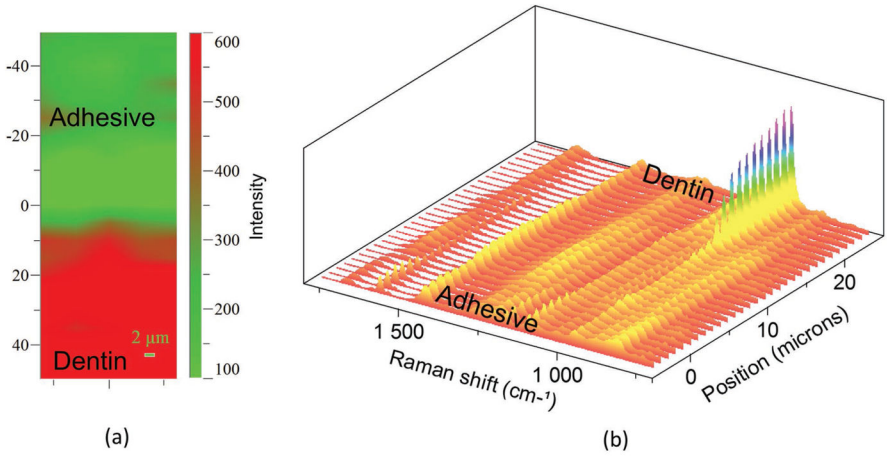

Figure 2.

a) Representative Raman *XY* imaging of the original a/d interface. b) The treated a/d interface specimens were analyzed using μRS and the absence of spectral features associated the mineral (PO_4^{-2} at 962 cm^{-1}) indicates ≈10 μm demineralization.

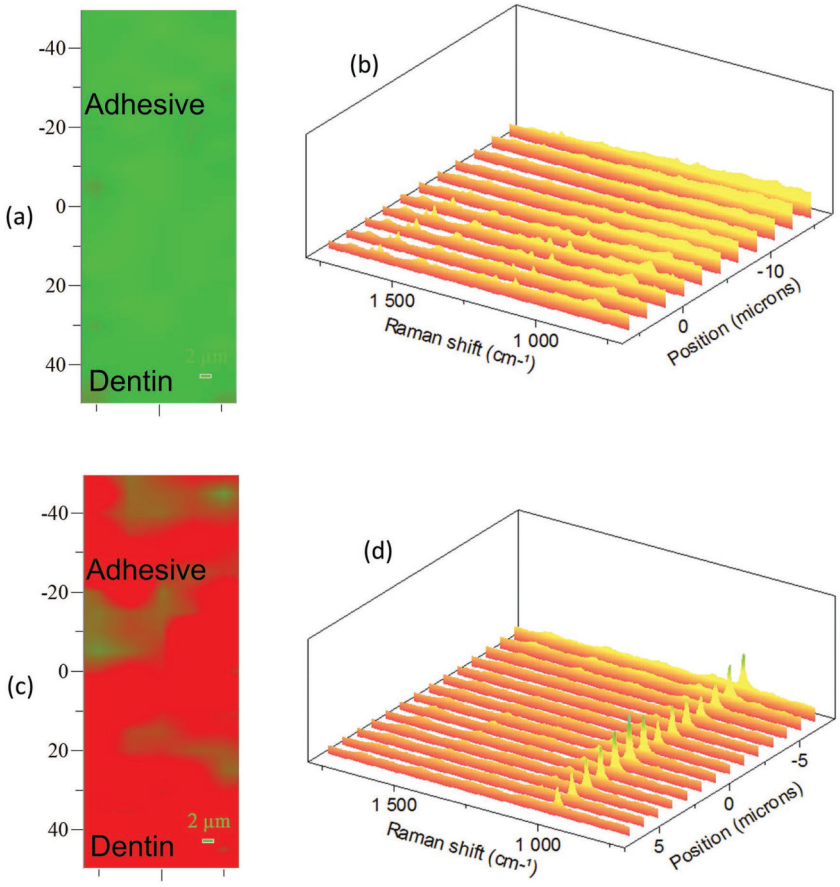

Figure 3.

a) Representative Raman *XY* imaging and b) the spectral analysis of the a/d interface following the additional etch. c) Raman *XY* imaging and d) the spectral analysis of the a/d interface after remineralization. The spectral features associated the mineral (PO_4^{-2} at 962 cm^{-1}) show up after the remineralization following the addition etch.

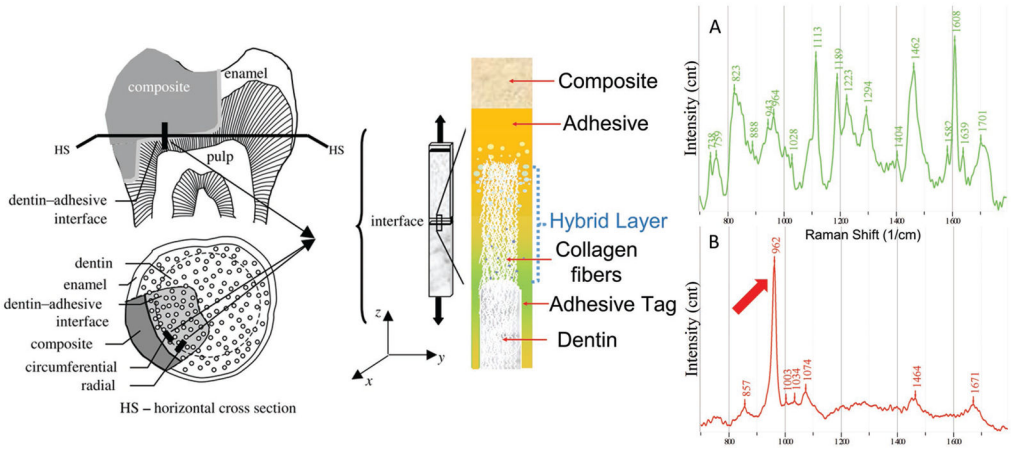

Scheme 1.

a) Adhesive/dentin interface - adapted with permission[40] and Raman spectrum of adhesive and b) Raman spectrum of dentin.